IJMCM
Spring 2020, Vol 9, No 2
DOI: 10.22088/IJMCM.BUMS.9.2.130

Original Article

Evaluation of miRNAs Related with Nuclear Factor Kappa B Pathway in Lipopolysaccharide Induced Acute Respiratory Distress Syndrome

Mustafa Azizoğlu[1], Lokman Ayaz[2*], Gülsen Bayrak[3], Banu Coşkun Yılmaz[3], Handan Birbiçer[1], Nurcan Doruk[1]

1. Mersin University, Faculty of Medicine, Department of Anesthesiology and Reanimation, Mersin, Turkey.
2. Trakya University, Faculty of Pharmacy, Department of Biochemistry, Edirne, Turkey.
3. Mersin University, Faculty of Medicine, Department of Histology & Embriyology, Mersin, Turkey.

Submmited 4 December 2019; Accepted 15 July 2020; Published 10 August 2020

This study aimed to determine the expression of nuclear factor kappa B (NF-κB) pathway related miRNAs in experimental acute respiratory distress syndrome (ARDS) induced by lipopolysaccharide (LPS) in rats, and to elucidate the underlying molecular mechanism. Twenty four sprague dawley rats were randomly divided into two groups; LPS (n = 12) and control (n = 12). Experimental ARDS was induced by intraperitoneal injection of *E. coli* LPS in LPS group. Intraperitoneal saline was administered in control group. Serum and lung samples were collected from both groups. Immunohistochemistry staining was performed for interleukin 1β (IL-1β), tumor necrosis factor α (TNF-α), CD 68, and caspase-3 in lung samples. Intensity of staining was scored as strong, moderate, weak, and no for evaluation of IL-1β and TNF-α. In addition, caspase-3 and CD68-positive stained cells were counted in sections. Expressions of 9 miRNAs were determined by quantitative real-time PCR in serum samples. IL-1β and TNF-α staining scores were significantly higher in the LPS group in comparison with the control group (P = 0.04 and P = 0.02, respectively). In addition, caspase-3 and CD68-positive stained cells were significantly higher in the LPS group (P = 0.02). Expressions of seven miRNAs were significantly changed in the LPS group in comparison with the control group. While six miRNAs (miR-7a-5p, miR-7b, miR-9a-5p, miR-21-5p, miR-29a-3p, and miR-138-5p) were up regulated, only miR-124-3p was down regulated. This study suggests that these miRNAs may have a role in the pathogenesis of ARDS related to NF-κB. However, this relationship needs to be examined in new studies by evaluation of pathways and target genes.

Key words: Acute respiratory distress syndrome, ARDS, microRNA, nuclear factor kappa B

Acute respiratory distress syndrome (ARDS) is a clinical condition that occurs as the result of direct or indirect lung injury, and is associated with high mortality. Its incidence is reported to be in the range of 2-70 per 100,000. The term 'diffuse alveolar damage' is used to describe the main histopathological feature of ARDS, though it may be associated with various causes (1). ARDS

*Corresponding author: Trakya University, Faculty of Pharmacy, Department of Biochemistry, Edirne, Turkey.
E-mail: lokmanayaz@yahoo.com

[DOI: 10.22088/IJMCM.BUMS.9.2.130]

progresses through three histopathologically distinct phases (exudative, proliferative, and fibrotic phases). Damage to the capillary endothelium and alveolar epithelium are initial findings, followed by interstitial edema, intraalveolar exudate, and fibrin accumulation. The remodeling phase is characterized by fibroblast and myeloblast proliferation. Fluid accumulation in the alveoli leads to protein deposition and hyaline membrane formation. All of these pathologies contribute to a clinical manifestation characterized by impaired alveolar gas exchange (1).

In the course of ARDS, inflammatory cascades are activated by the release of numerous cytokines and chemokines, most of which are involved in transcriptional regulation of nuclear factor kappa-beta (NF-κB) (2-4). Previous research has demonstrated that lipopolysaccharide (LPS) can activate NF-κB, a nuclear transcription factor that plays a key role in the modulation of inflammatory and immune responses (5). Under physiological conditions, NF-κB heterodimers, mainly p50/p65, remain in an inactive form in the cell cytoplasm via their linkage to an inhibitor of the κB protein (IκB) (6). However, once activated, IκB is phosphorylated by IκB kinase (IKK) and is rapidly degraded, releasing p50/p65 heterodimers that are translocated to the nucleus where they modulate various inflammatory mediators, such as interleukin-1β (IL 1β), interleukin-6 (IL-6) and tumor necrosis factor-α (TNF-α) (7).

Moreover, these cytokines trigger the release of anti-inflammatory cytokines such as IL-4, IL-10, and IL-13, which inhibit NF-κB activity (8, 9).

MicroRNAs (miRNAs) comprise a group of small, non-coding RNAs that regulate gene expression by binding to specific target sites on mRNA to either repress or degrade targets. In recent years, it has been reported that miRNAs have an important role in a number of basic physiological and pathological processes such as cell proliferation, differentiation, migration, apoptosis, metabolism, organogenesis, oncogenesis, immune response, and inflammation. Most importantly, emerging evidence suggest that miRNAs play crucial roles in inflammation responses (10), as well as in acute lung injury and ARDS (11). These processes are also known to be regulated by NF-κB, and therefore miRNAs may be involved in the development of ARDS (12-17). In a rat model of ARDS, miRNA profiling of lung tissue demonstrated altered expression of multiple miRNAs compared to control tissues (17). There is currently no effective treatment recommended for ARDS, and supportive care is usually implemented after diagnosis (18).

Elucidating the role of miRNAs in pathophysiology may be beneficial both in the diagnosis and treatment of many diseases. The aim of the present study was to investigate changes in serum expression levels of nine miRNAs associated with NF-κB pathway (according to miRWalk and targetscan databases) in an experimental model of ARDS.

Materials and methods

Study design and induction of experimental ARDS

After receiving approval from the Mersin University Animal Experiments Local Ethics Committee (2016/19), twenty four male Sprague-Dawley rats aged 10-12 weeks and weighing 205-305 g were included in the study. The rats were randomly divided into 2 groups, the LPS (n = 12) and control (n=12) groups. International guidelines were observed during the maintenance and testing of experimental animals. Experimental ARDS was induced in LPS group by intraperitoneal injection of *Escherichia coli* LPS (5 mg/kg) (19). Intraperitoneal saline was administered to the rats in the control group. After 24 h, all of the rats were killed by intraperitoneal injection of ketamine (Pfizer İlaçları Ltd. Şti, Istanbul Turkey) and xylazine (Rompun, Bayer) mixture (2:1, 0.3

[DOI: 10.22088/IJMCM.BUMS.9.2.130]

mL/rat). Blood samples were obtained from the abdominal aorta for miRNAs analyzes, and lungs were removed from the animals.

Histological analysis and immunohistochemistry

Lung tissue samples were fixed in 10% neutral buffered formalin for 24 h, dehydrated in a graded ethanol series, and embedded in paraffin. Tissue blocks were sectioned into 5 µm-thick slices by rotary microtome (Leica RM2255, Leica, Germany). After staining with hematoxylin and eosin (H&E), pathological changes in the lung tissues were observed using a light microscope (BX50; Olympus, Tokyo, Japan). A lung injury score was assigned by a blinded pathologist based on a 0 to 4-point scale according to a combined assessment of inflammatory cells infiltration in the airspace or alveolar congestion, alveolar wall thickness, vessel wall, hemorrhage, and hyaline membrane formation, where a score of 0 represented no damage; l represented mild damage; 2 represented moderate damage; 3 represented severe damage, and 4 represented very severe histological changes (20).

For immunohistochemistry staining, sections were deparaffinized. After deparaffinization, the sections were rehydrated, antigen-retrived (Tris-EDTA buffer, Abcam, Cambridge, UK), and blocked with normal goat serum. Then the sections were incubated with primary antibodies against IL-1β (1/100, Abcam, ab9787, Cambridge, UK), TNF-α (1/100, Abcam, ab6671, Cambridge, UK), caspase-3 (1/100, Cell Signaling Technology, 9661, Massachusetts, USA), and CD 68 (1/100, Abcam, ab31630, Cambridge, UK) overnight at 4 ^{0}C. Thereafter sections of IL-1β, TNF-α, caspase-3 were incubated with goat anti-rabbit secondary antibody (Chemicon, MerckMillipore, AP132B, Massachusetts, USA) for 90 min. The sections stained with anti-CD68 antibody were incubated with anti-mouse secondary antibody (Millipore, AP124B, Massachusetts, USA) for 90 min. Then, horseradish peroxidase (HRP, Millipore, SA202, Massachusetts, USA) was added for 10 min in dark. 3,3- diaminobenzidine substrate (DAB, Abcam, Cambridge, UK) was used to detect enzymatic activity, and then nuclei were counterstained with hematoxylin except sections of caspase-3. The sections were mounted with entellan (Merck, Darmstadt, Germany). Images were taken with the digital camera (Nikon Coolpix5000, Tokyo, Japan) connected to a light microscope (Olympus BX50, Tokyo, Japan). For IL-1β and TNF-α immunohistochemical evaluations, two sections from each animal was examined at magnification X20, and the intensity of staining was scored as strong (++++), moderate (+++), weak (++) and no (+). For caspase-3 and CD68 immunohistochemical evaluations, two sections from each animal were examined at magnification X40, and positive stained cells were counted in five different areas.

Serum preparation and RNA isolation and cDNA synthesis

Serum samples were collected by centrifuging blood samples at 4,000 rpm for 15 min within 2 h of collection. The supernatants were transferred into clean microcentrifuge tubes, followed by a second high-speed centrifugation at 13,000 rpm for 5 min at 10 °C to remove cell debris and fragments. The serum samples were aliquoted and stored at -80 °C until RNA extraction. miRNA was extracted using miRCURY™ Isolation Kit (Exiqon, Woburn, MA, USA) according to the manufacturer's instructions, and then stored at -80 °C for further processing. Isolated miRNA samples were then converted to complementary DNA (cDNA) using a miScript II Reverse Transcription Kit (Qiagen, Maryland, USA). All reactions were performed as specified according to the manufacturer's protocol. cDNA samples were stored at -80 °C until RT-PCR analysis.

Pre-amplification of cDNA and quantitative real-time PCR analysis (qRT-PCR)

For pre-amplification, 10 µL cDNA samples were transferred into a clean 96-well plate and 40

[DOI: 10.22088/IJMCM.BUMS.9.2.130]

µL RNase-free water were added and mixed by pipetting up and down five to six times. One-fifth of the diluted RT product (2 µL) was pre-amplified using miScript PreAMP Primer Mix (Qiagen, Maryland, USA) and miScript Microfluidics Universal Primer in a 10 µL PCR volume. QRT-PCR was performed using miScript EvaGreen PCR kit (Qiagen, Maryland, USA). Gene expression profiles were generated using the custom miScript miRNA PCR array for the following microRNAs: miR-7a-5p, miR-7b, miR-21-5p, miR-29a-3p, miR-138-5p, miR-9a-5p, miR-126b, miR-504, and miR-124-3p (Qiagen, Maryland, USA) according to manufacturers' instructions. RT-PCR was done using a high-throughput BioMark RT-PCR system (Fluidigm, South San Francisco, CA, USA) under the following cycling conditions: 10 min at 95 °C, 40 cycles of 15 s at 94 °C, 30 s at 55 °C, and 30 s at 70 °C. Each array also included reverse transcription controls (miRTC), positive PCR controls (PPC), and a panel of control miRNAs for quality control as well as normalization. We chose *Caenorhabditis elegans* miR-39 as the internal control for RNA input; miRNAs expression data were normalized according to the global mean normalization strategy. The relative expression of miRNAs was calculated with the comparative delta delta CT (ΔΔCT) method. Fold change (FC) was calculated as $2^{-\Delta\Delta CT}$ (21).

Statistical analysis

Statistical analyzes were performed with SPSS software package, version 17.0 for Windows (SPSS Inc., Chicago, IL, USA). Relative gene expression in the control and LPS groups was analyzed using QIAGEN relative expression software (www. qiagen.com/ fo/ shop/ genes- and- pathways/ data-analysis- center- overview- page/). Results were expressed as mean ± standard error (SE). For IL-1β, TNF-α, caspase-3, and CD68 histological data, statistical analysis was performed using Mann-Whitney U test to detect differences between the groups. A P-value<0.05 was considered significant.

Results

Clinical examination

Respiratory distress was observed in the LPS group, but all of the animals were alive at 24 h after intraperitoneal LPS injection.

Histological examination of lungs and immune-histochemistry

To evaluate the rat model of LPS-induced ARDS, we performed the H&E staining of lung tissues and assigned a lung injury score system to evaluate the histological changes. As shown in Figures 2 and 3, in comparison with the control group (Figure 1), LPS induced severe lung destruction including alveolar hemorrhage, mass inflammatory cell infiltration, severe pulmonary edema, and alveolar collapse (P <0.05 in all cases). IL-1β and TNF-α staining scores were significantly

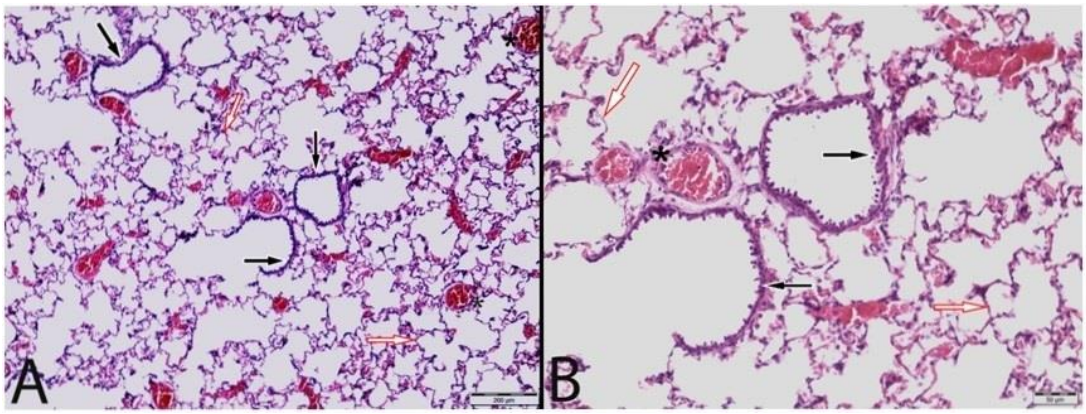

Fig. 1. Histological examination of lungs in control group. Normal bronchial epithelium, wall and lumen (black arrow), blood vessels (asterisk), alveolar wall and lumen (white arrow) were observed after H&E staining. A x4, B x10 magnification.

[DOI: 10.22088/IJMCM.BUMS.9.2.130]

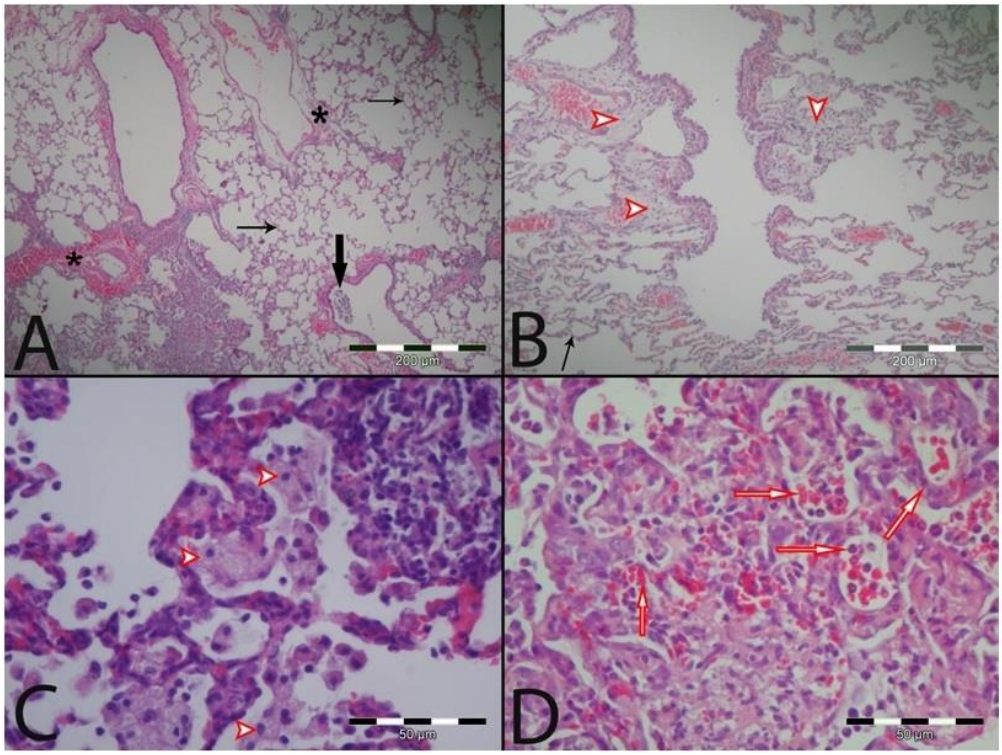

Fig. 2. Histological changes in lung tissues of LPS-induced phase 1 ARDS rats. Lung tissues were evaluated by H&E staining and use of a lung injury score system (ARDS phase 1). Normal alveolar wall (thin black arrow), sloughed cell and infiltration in the bronchial lumen (thick black arrow), perivascular extravasation (asterisk), foamy macrophages (arrowhead), erythrocytes and the neutrophil leukocyte infiltration in the alveolar lumen (white arrow) were observed after H&E staining. A and B x10, C and D x40, magnification.

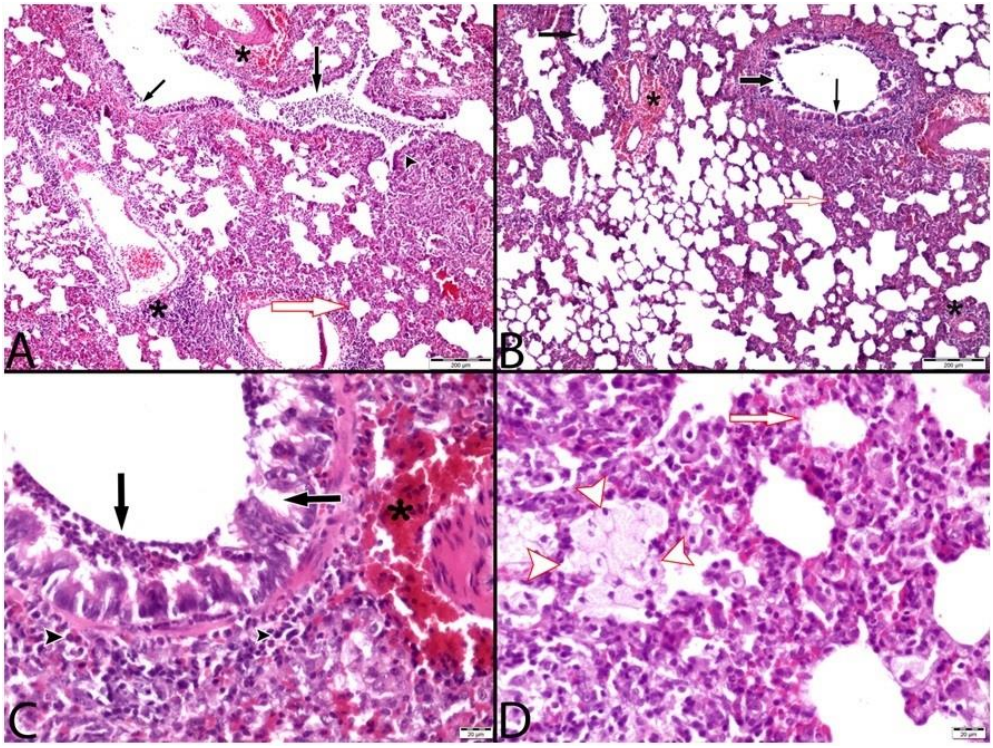

Fig. 3. Histological changes in lung tissues of LPS-induced phase 2 ARDS rats. Lung tissues were evaluated by H&E staining and use of a lung injury score system (ARDS phase 2). Sloughed cell from the epithelium, erythrocytes and infiltration in the bronchial lumen and the disorganized epithelium (black arrow), perivascular extravasation and cuffing (asterisk), thickened bronchial wall (black arrowhead), thickened alveolar wall (white arrow), foamy macrophages (white arrowhead) were observed after H&E staining. A and B x4, C and D x20, magnification.

[DOI: 10.22088/IJMCM.BUMS.9.2.130]

higher in the LPS group in comparison with the control group (P=0.04, and P = 0.02, respectively, Figures 4 and 5). In addition, caspase-3 and CD68-positive stained cells were significantly higher in the LPS group (P=0.02, for both parameters, Figures 6 and 7). miR-7b, miR-9a-5p, miR-21-5p, miR-29a-3p, and miR-138-5p were up regulated, while miR-124-3p was down regulated in the LPS group in comparison with the control group (Table1).

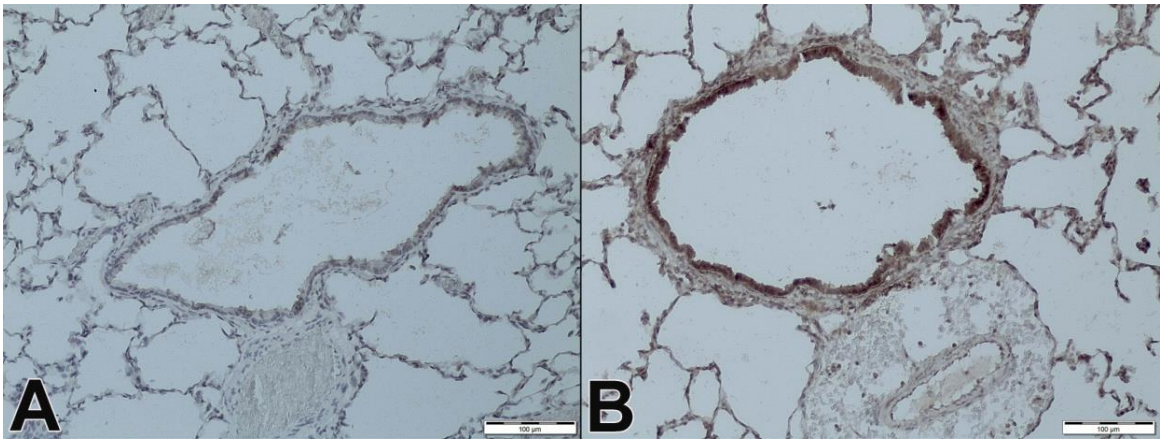

Fig. 4. IL-1β staining. A, control group, B, study group. x100.

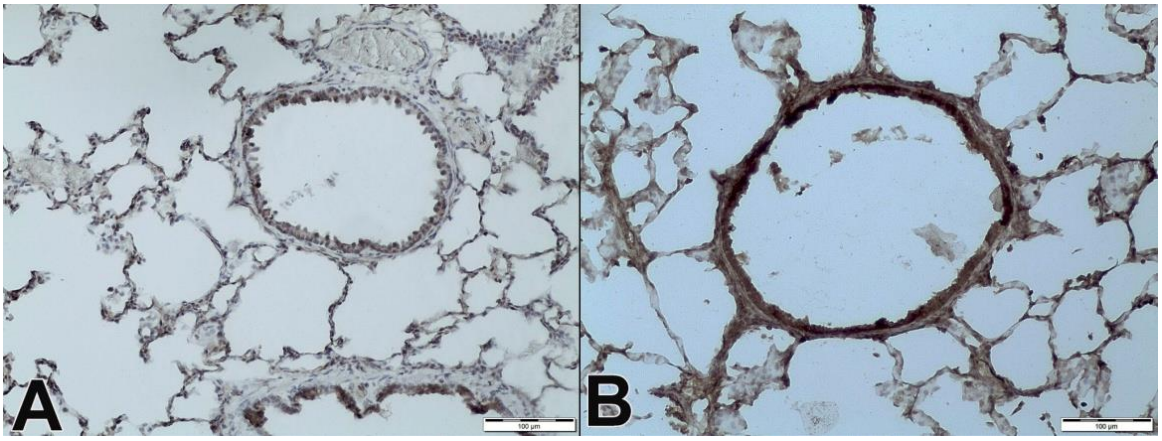

Fig. 5. TNF-α staining. A, control group, B, study group. x100.

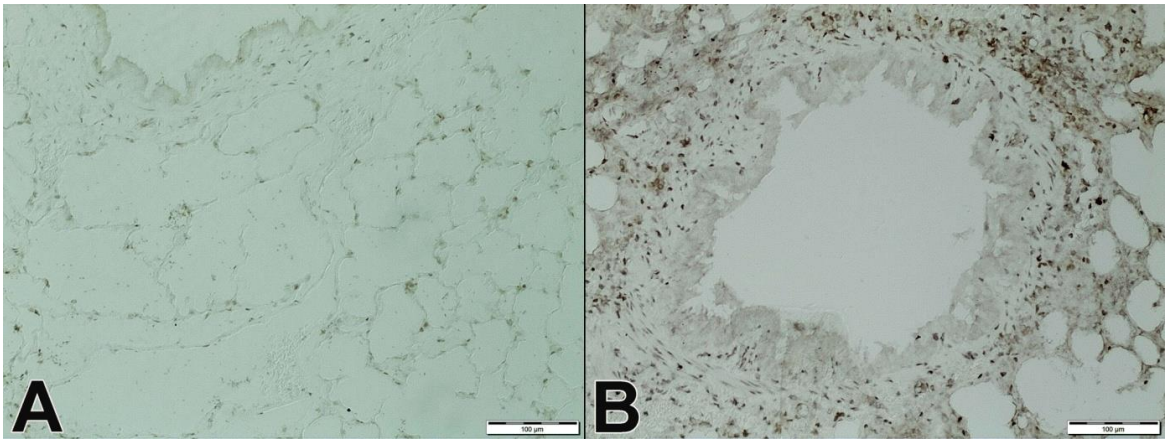

Fig. 6. Active caspase-3 staining. A, control group, B, study group. x100.

[DOI: 10.22088/IJMCM.BUMS.9.2.130]

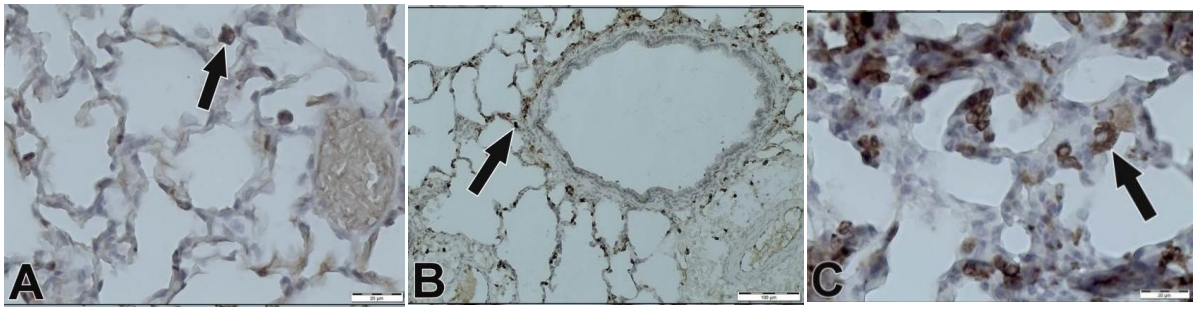

Fig. 7. CD68 staining. A, control group, B and C, study group, positive stained macrophages (black arrow). A and C; x400, B; x100.

Table 1. Fold change and P values of LPS-induced ARDS group compared to the control group.

miRNAs	Fold change	P value
miR-7a-5p	1.641±0,68	0.001*
miR-7b	1.7772±0,69	0.001*
miR-9a-5p	1.7937±0,3	0.0001*
miR-21-5p	1.7396±0,59	0.00001*
miR-29a-3p	1.3368±0,49	0.0224*
miR-124-3p	-2.2339±0,33	0.0003*
miR-126b	-1.2251±0,67	0.640
miR-138-5p	2.1703±0,36	0.000004*
miR-504	-1.3199±0,45	0.120

*P < 0.05

Discussion

In the present study, we observed a significant up regulation of miR-21-5p in the ARDS group in comparison with the control group. It is known that miR-21 is functionally related and contribute to NF-κB signaling, an important pathway for innate and adaptive immunity and inflammation (22). Furthermore, miR-21 has been shown to play multiple roles in different pulmonary diseases, such as idiopathic pulmonary fibrosis and pulmonary arterial hypertension, by targeting several immune receptors and cytokines, including IL-12 and mothers against decapentaplegic homolog 7 (SMAD7) (23). It is known that miR-21 targets the phosphatase and tensin homolog (*PTEN*) gene (http://zmf.umm.uni-heidelberg.de/apps/zmf/mirwalk 2/). *PTEN* is a known inhibitor of protein kinase B (AKT) phosphorylation that promotes NF-κB activation and enhances tumorigenesis. Thus, miR-21 works within the inflammation-transformation positive feedback loop by down regulating *PTEN* expression to increase NF-κB activity. In the ARDS group, up regulation of miR-21-5p may result in NF-κB activation. In an LPS-induced acute lung injury (ALI) mouse model with miR-7 knockdown mice (miR-7KD) developed by Zhao et al (24), miR-7 deficiency reduced the expression of NF-κB and phosphorylation of AKT and extracellular signal-regulated kinase (ERK). In addition, levels of pro-inflammatory factors TNF-α, IL-1β, and IFN-γ in bronchoalveolar lavage samples from the LPS-treated miR-7KD group were significantly lower on day 3 in comparison with those in the control group. These results suggested that the evident effect of miR-7 deficiency on the pathology of ALI was closely correlated to altered transduction of the NF-κB, AKT, and ERK signaling pathways. Also, it has been reported that miR-7b is up regulated in ALI-ARDS model (25). The present study showed that expression of miR-7a-5p and miR-7b was up regulated in ARDS group. Up regulation of these

[DOI: 10.22088/IJMCM.BUMS.9.2.130]

miRNAs may cause ARDS by increasing transduction of these signaling pathways.

miR-9 targets the *NFKB1/p105* gene, and this interaction is implicated in the attenuation of NF-κB signaling. miR-9 is induced by LPS via myeloid differentiation primary response protein MyD88 and NF-κB (25). Induction of miR-9 is also mediated by the pro-inflammatory cytokines IL-1b and TNF-α (26). Otsuki et al. (27) demonstrated that miR-9 was significantly up regulated by LPS in a rat LPS-induced ALI model. In the present study, we found that miR-9a-5p was up regulated in the LPS-induced ARDS model. In addition, IL-1β and TNF-α staining scores were significantly higher in the ARDS group in comparison with the control group. miR-9 may have contributed to the development of ARDS by inducing NF-κB signaling pathway.

Guo et al. (28) reported that miR-124 expression was up regulated in mice tissues in LPS-induced ALI. In this study, we observed that the expression of serum miR-124-3p was down regulated in the LPS-induced ARDS rat model. miR-124a is the first reported miRNA targeting a member of the IkB family (IkB epsilon) though the biological importance of this regulation remains unclear (29). According to the Targetscan database (http://www.targetscan.org/vert_71), TNF receptor-associated factor 6 (*TRAF6*) is one of the target genes of miR-124. miR-124 may down regulate *TRAF6* to suppress the activity of *NF-κB*. However, miR-124-3p was down regulated in the present study, which may have led to an increase in *TRAF6* levels and thus *NF-κB* activation.

We also observed that miR-29a-3p was up regulated in ARDS group. According to the Targetscan database, miR-29a targets NF-κB repressing factor (*NKRF*). MiR-29a down regulates *NKRF*, and thereby promotes *NF-κB* activation. Moreover, miR-29a inhibition or *NKRF* up regulation in ARDS rats led to reduced *NF-κB* target gene expression and may have attenuated ARDS. In this study, we observed an approximately 2-fold upregulation in miR-138-5p in the ARDS group. Requenez-Contreras et al. (30) determined that in human cell culture, miR-138 significantly decreased v-rel avian reticuloendotheliosis viral oncogene homolog A (*RELA*) expression at mRNA level in comparison with non-transfected cells or miRNA hairpin control. Additionally, they reported significant down regulation for NF-κB/p65 protein expression after transfection of pLVX-miR-138 vector in AD-293 cells as compared with controls. These results confirm that *NF-κB*/*p65* is a direct target of miR-138 in AD-293 cells. They also found that miR-138 inhibits the expression of canonical NF-κB/p65 target genes in U937 cells. They observed that miR-138 down regulates the expression of *TNF-α* and *IL-6* mRNA and inhibits the release of these pro-inflammatory cytokines in LPS-stimulated cells. The contradictory results obtained in the present study may be related to the different species studied and the assessment of serum responses rather than levels in cell culture. miR-138 might also function as an intracellular modulator of responses initiated by the LPS/TLR4 signaling pathway.

In conclusion, miR-7a-5p, 7b, 9a-5p, 21-5p, 124-3p, and miR-138-5p may have caused NF-κB-mediated ARDS, and serum levels of these miRNAs may be used as a biomarker in the diagnosis of ARDS. Targeted silencing or replacement of these mi-RNAs may also be used in the treatment of ARDS. Further studies are needed to evaluate the possible pathways associated with these expressed miRNAs. The results of the present study may provide a basis for future research.

Acknowledgments

This study was supported by Mersin University Scientific Researsch Project Unit (Grant: 2016-2-AP3-1914).

Conflict of interest

Authors declare no conflict of interest.

[DOI: 10.22088/IJMCM.BUMS.9.2.130]

References

1. Tomashefski JF, Jr. Pulmonary pathology of acute respiratory distress syndrome. Clin Chest Med 2000;21:435-66.

2. Fan J, Ye RD, Malik AB. Transcriptional mechanisms of acute lung injury. Am J Physiol Lung Cell Mol Physiol 2001;281:L1037-50.

3. Blackwell TS, Christman JW. The role of nuclear factor-kappa B in cytokine gene regulation. Am J Respir Cell Mol Biol 1997;17:3-9.

4. Puneet P, Moochhala S, Bhatia M. Chemokines in acute respiratory distress syndrome. Am J Physiol Lung Cell Mol Physiol 2005;288:L3-15.

5. Hayden MS, Ghosh S. Shared principles in NF-kappaB signaling. Cell 2008;132:344-62.

6. Collins T, Cybulsky MI. NF-kappaB: pivotal mediator or innocent bystander in atherogenesis? J Clin Invest 2001;107:255-64.

7. Lv H, Yu Z, Zheng Y, et al. Isovitexin Exerts Anti-Inflammatory and Anti-Oxidant Activities on Lipopolys-accharide-Induced Acute Lung Injury by Inhibiting MAPK and NF-kappaB and Activating HO-1/Nrf2 Pathways. Int J Biol Sci 2016;12:72-86.

8. Ward PA. Acute lung injury: how the lung inflammatory response works. Eur Respir J Suppl 2003;44:22s-3s.

9. Husain AN. The Lung. In: Kumar V, Abbas A, Fausto N, et al., editors. Robbins and Cotran Pathologic Basis of Disease. 8th ed. Philadelphia: Elsevier; 2009. p. 677-737.

10. Deshpande DA, Dileepan M, Walseth TF, et al. MicroRNA Regulation of Airway Inflammation and Airway Smooth Muscle Function: Relevance to Asthma. Drug Dev Res 2015;76:286-95.

11. Cao Y, Lyu YI, Tang J, et al. MicroRNAs: Novel regulatory molecules in acute lung injury/acute respiratory distress syndrome. Biomed Rep 2016;4:523-7.

12. Zeng Z, Gong H, Li Y, et al. Upregulation of miR-146a contributes to the suppression of inflammatory responses in LPS-induced acute lung injury. Exp Lung Res 2013;39:275-82.

13. Cai ZG, Zhang SM, Zhang Y, et al. MicroRNAs are dynamically regulated and play an important role in LPS-induced lung injury. Can J Physiol Pharmacol 2012;90:37-43.

14. Staszel T, Zapala B, Polus A, et al. Role of microRNAs in endothelial cell pathophysiology. Pol Arch Med Wewn 2011;121:361-6.

15. Magenta A, Greco S, Gaetano C, et al. Oxidative stress and microRNAs in vascular diseases. Int J Mol Sci 2013;14: 17319-46.

16. Carissimi C, Fulci V, Macino G. MicroRNAs: novel regulators of immunity. Autoimmun Rev 2009;8:520-4.

17. Huang C, Xiao X, Chintagari NR, et al. MicroRNA and mRNA expression profiling in rat acute respiratory distress syndrome. BMC Med Genomics 2014;7:46.

18. Calfee CS, Matthay MA. Nonventilatory treatments for acute lung injury and ARDS. Chest 2007;131:913-20.

19. Fodor RS, Georgescu AM, Cioc AD, et al. Time- and dose-dependent severity of lung injury in a rat model of sepsis. Rom J Morphol Embryol 2015;56:1329-37.

20. Parsey MV, Tuder RM, Abraham E. Neutrophils are major contributors to intraparenchymal lung IL-1 beta expression after hemorrhage and endotoxemia. J Immunol 1998;160:1007-13.

21. Pfaffl MW. A new mathematical model for relative quantification in real-time RT-PCR. Nucleic Acids Res 2001;29:e45.

22. Ma X, Becker Buscaglia LE, Barker JR, et al. MicroRNAs in NF-kappaB signaling. J Mol Cell Biol 2011;3:159-66.

23. Sessa R, Hata A. Role of microRNAs in lung development and pulmonary diseases. Pulm Circ 2013;3:315-28.

24. Zhao J, Chen C, Guo M, et al. MicroRNA-7 Deficiency Ameliorates the Pathologies of Acute Lung Injury through Elevating KLF4. Front Immunol 2016;7:389.

25. Vaporidi K, Vergadi E, Kaniaris E, et al. Pulmonary microRNA profiling in a mouse model of ventilator-induced lung injury. Am J Physiol Lung Cell Mol Physiol 2012;303:L199-207.

26. Bazzoni F, Rossato M, Fabbri M, et al. Induction and regulatory function of miR-9 in human monocytes and neutrophils exposed to proinflammatory signals. Proc Natl Acad Sci U S A 2009;106:5282-7.

27. Otsuki T, Ishikawa M, Hori Y, et al. Volatile anesthetic sevoflurane ameliorates endotoxin-induced acute lung injury via microRNA modulation in rats. Biomed Rep 2015;3:408-12.

28. Guo ZL, Ren T, Xu L, et al. The microRNAs expression changes rapidly in mice lung tissue during lipopolysaccharide-induced acute lung injury. Chin Med J (Engl) 2013;126:181-3.

29. Lindenblatt C, Schulze- Osthoff K, Totzke G. Ikappa Bzeta expression is regulated by miR- 124 a. Cell Cycle 2009;

[DOI: 10.22088/IJMCM.BUMS.9.2.130]

8:2019-23.

30. Requenez-Contreras JL, Lopez-Castillejos ES, Hernandez-Flores R, et al. MiR-138 indirectly regulates the MDR1 promoter by NF-kappaB/p65 silencing. Biochem Biophys Res Commun 2017;484:648-55.

[DOI: 10.22088/IJMCM.BUMS.9.2.130]